

What Caused The Increase of Tropical Cyclones In The Western North Pacific During The Period of 2011-2020?

Haili Wang

South China Sea Institute of Oceanology Chinese Academy of Sciences

Chunzai Wang (✉ cwang@scsio.ac.cn)

South China Sea Institute of Oceanology Chinese Academy of Sciences <https://orcid.org/0000-0002-7611-0308>

Research Article

Keywords: Tropical cyclone, Western North Pacific, Pacific Decadal Oscillation

Posted Date: August 26th, 2021

DOI: <https://doi.org/10.21203/rs.3.rs-834680/v1>

License:  This work is licensed under a Creative Commons Attribution 4.0 International License.

[Read Full License](#)

Abstract

Based on satellite era data after 1979, we find that the tropical cyclone (TC) variations in the Western North Pacific (WNP) can be divided into three-periods: a high-frequency period from 1979-1997 (P1), a low-frequency period from 1998-2010 (P2), and a high-frequency period from 2011-2020 (P3). Previous studies have focused on WNP TC activity during P1 and P2. Here we use observational data to study the WNP TC variation and its possible mechanisms during P3. Compared with P2, more TCs during P3 are due to the large-scale atmospheric environmental conditions of positive relative vorticity, negative vertical velocity and weak vertical wind shear. Warmer SST is found during P3, which is favorable for TC genesis. The correlation between the WNP TC frequency and SST shows a significant positive correlation around the equator and a significant negative correlation around 36°N, which is similar to the warm phase of the Pacific Decadal Oscillation (PDO). The correlation coefficient between the PDO and TC frequency is 0.71, significant at 99% confidence level. The results indicate that the increase of the WNP TC frequency during 2011-2020 is associated with the phase transition of the PDO and warmer SST. Therefore, more attention should be given to the warmer SST and PDO phase when predicting WNP TC activity.

Introduction

Tropical cyclone (TC) is one of the most intense weather systems in the world. A TC is called a typhoon when its wind speed exceeds 34 knots in the Western North Pacific (WNP). The WNP basin (0°-30°N, 100°E-180°) exhibits a high level of TC activity and is the most active region globally. About 26 TCs enter the WNP basin each year, leading to huge loss of life and property (Zhang et al., 2009, Wang et al., 2021). Many studies point out that an increasing pattern in TC-induced damages over the past several decades (Knutson et al., 2010; Mendelsohn et al., 2012; Peduzzi et al., 2012). A better understanding of how the behavior of TCs may change (such as their frequency) has scientific and socio-economic values. Under the background of global warming, whether the number of TCs is increasing has attracted much attention.

Great efforts have been put in improving our understanding of changes in TC activity (Zhao and Wang, 2019; Liu et al., 2019, Yamaguchi et al., 2020). Numerous studies have shown the favorable large-scale conditions for TC formation (Bister and Emanuel, 1997; Ritchie and Holland, 1997; Molinari et al., 2000; Nolan et al., 2007; Vu et al., 2020; Walsh et al., 2020). Several general conducive conditions are: (a) warm sea surface temperature (SST); (b) weak vertical wind shear; (c) high relative humidity; and (d) large vorticity. Understanding the environmental conditions that cause changes in TC genesis is very important for practical applications (such as TC forecast).

TCs show significant variability at multiple time scales, due to various climate forcing (Wang and Chan 2002; Vecchi and Soden 2007; Kim et al. 2008; Zhan et al. 2012; Li and Zhou 2013; Lin and Chan 2015; Wang et al. 2015; Mei and Xie 2016). The Madden–Julian Oscillation (MJO) with 30–90 day period can regulate WNP TC activity (Li and Zhou, 2013; Liu et al., 2021; Wang et al., 2018; Zhao and Wang, 2019). In the WNP basin, the active phase of the MJO enhances the local convection, which in turn leads to the

increase in TC activity in the basin. Quasi-biweekly oscillation (QBWO) is another intra-seasonal mode, but with a more localized effect, that also affects WNP TC activity (Li and Zhou 2013). The El Niño-Southern Oscillation (ENSO) is known as the main phenomenon occurring at inter-annual time scales (Trenberth and Caron 2000; Timmermann et al. 2018). ENSO has significant impacts on WNP TCs (Kim et al., 2011). Zhao and Wang (2016, 2019) examine a stronger inter-annual relationship between ENSO and TCs in the WNP during the boreal summer from 1998 to 2015. The correlation is 0.60 at 95% confidence level. At decadal time scales, many factors affecting the TC frequency have already been suggested. The researchers mainly focus on the following factors: (a) the strengthened western North Pacific subtropical high (Liu and Chan, 2020); (b) the anomalous westward WNP SST gradient (Choi et al., 2015); (c) phase shifts of the Pacific Decadal Oscillation (PDO) (Zhao and Wang, 2016); (d) the Inter-decadal Pacific Oscillation (He et al., 2015; Zhao et al., 2018), and also (e) the Atlantic Multi-decadal Oscillation (AMO) (Zhang et al., 2020; Zhang et al., 2017). The potential mechanisms of WNP TC decadal changes remain to be studied.

Most studies suggest that the frequency of WNP TCs decreased from 1979 to 2010 (Tu et al., 2009; Yokoi and Takayabu, 2013; Hsu et al., 2014). Few studies have examined the change of TC activity from 2010 to 2020. Most of the previous analyses on TCs focus on the first or the second half of the year, or a certain period of the year, and the number of TCs throughout the year is less covered in previous studies. With global warming and the emergence of various extreme weather phenomena, how did the TC frequency per year change during 2010–2020 compared to the pre-2010 decades? And what caused those changes? To our knowledge, these issues have not been explained in previous studies. Here we investigate the possible reasons associated with the changes in the WNP TC frequency during 2010–2020 based on observations and reanalysis data.

The aim of this paper is to explore the change of the WNP TC frequency, and the corresponding large-scale atmospheric changes and oceanic SST changes. The rest of this paper is organized as follows. Section 2 describes the data used in this study. The TC increase is illustrated in Sect. 3. In Sect. 4, we explore the possible influences of large-scale atmospheric environment and ocean conditions associated with TC increase. The main interrelated discussion and conclusions are presented in Sect. 5.

Data

2.1 TC data

The TC best-track data, including the TC intensity, latitude and longitude, are from the United States Joint Typhoon Warning Center (JTWC). The selected period for the present study is the period after the satellite era from 1979 to 2020 (<https://www.ncdc.noaa.gov/ibtracs/index.php?name=ib-v4-access>). In this study, we focus on the TC frequency throughout the year (from January to December). The TC frequency in this study is calculated over the whole WNP region. The WNP domain (0° – 30° N, 100° E– 180°) is divided into $5^{\circ} \times 5^{\circ}$ resolution grids. TC genesis positions are counted for each grid box. The first position of a TC

recorded in JTWC is defined as the TC genesis location. Student's t test is performed to test statistical significance.

2.2 Atmospheric and SST data

The monthly mean atmospheric fields (e.g., winds) are obtained from the United States National Centers for Environmental Prediction and National Center for Atmospheric Research (NCEP/NCAR) monthly Reanalysis II dataset with a $2.5^\circ \times 2.5^\circ$ grid (Kalnay et al. 1996) (<https://psl.noaa.gov/data/gridded/>). The monthly mean SST is taken from the United States National Oceanic and Atmospheric Administration (NOAA) Extended Reconstruction SST version 5 (ERSSTv5) with a resolution of $2^\circ \times 2^\circ$ (Huang et al. 2017).

2.3 Selection of ENSO events

The Niño 3.4 SST index is calculated from the HadISST1 dataset (Rayner et al. 2003) (https://psl.noaa.gov/gcos_wgsp/Timeseries/Nino34/). The Oceanic Niño Index (ONI) from the Climate Prediction Center is used to distinguish El Niño and La Niña years based on a 0.5°C threshold. (https://origin.cpc.ncep.noaa.gov/products/analysis_monitoring). The years with SST anomalies larger (less) than 0.5°C (-0.5°C) during the late season (October to December) are defined as El Niño (La Niña) years. The other years are considered as neutral years. Detailed classifications are shown in Table 1. P1, P2 and P3 represent the periods of 1979–1997, 1998–2010 and 2011–2020, respectively.

Table 1
The list of El Niño years, La Niña years and neutral years during P2(1998–2010)and P3 (2011–2020)

	P2(1998–2010)	P3(2011–2020)
El Niño years	2002 2004 2006 2009	2014 2015 2018
La Niña years	1998 1999 2000 2007 2010	2011 2016 2017 2020
Neutral years	2001 2003 2005 2008	2012 2013 2019

Tc Frequency Changes

The present work focuses on the total number of WNP TCs each year (from January to December), and all analyses use the annual mean data. The time series of the WNP TC numbers are displayed in Fig. 1. Based on the variations, we divide 1979–2020 into three epochs, with turning points in 1998 and 2010, respectively. The reason for choosing these two years as turning points is that the number of TCs generated in the WNP is the least in the two years. Moreover, 1998 is approximately the PDO phase transition year (Zhao and Wang, 2016). Compared with P2, there is a significant and abrupt increase in the WNP TC frequency during P3 (Fig. 1). Since the TC frequency between P1 and P2 has been previously studied (e.g., Zhao and Wang, 2016, 2019; Choi and Kim, 2019; Zhao et al., 2021), this study explores the reasons for the WNP TC frequency rise during P3 compared to P2.

Figure 2 shows that more TCs can be found during P3 than during P2. The difference between P2 and P3 is 3.3. It is shown that the major difference between P2 and P3 is due to the significant differences during neutral and La Niña years. In La Niña years, the average TC number in P2 (P3) is about 20 (24). In neutral years, the average TC counts in P2 (P3) are about 23.5 (28.3). In El Niño years, 25.25 (26.33) TCs are observed during P2 (P3). Figure 2 also shows that there is more TC generation in La Niña years and neutral years during P3 compared to P2. Furthermore, most TCs form in neutral years than in La Niña and El Niño years in P3, while most TCs are in El Niño years during P2. It is shown that there is no significant change of the TC frequency between P2 and P3 in El Niño years.

Large-scale Climate Patterns Related To Tc Frequency Changes

4.1 Differences in atmospheric and SST conditions between P2 and P3

Figure 3 shows that TCs in the northwest, southeast, and central areas increase significantly during P3 compared to P2. There is a slight reduction between 10° - 18° N and 155° - 160° E. More TCs can be observed over the South China Sea during P3. The genesis of TCs is generally influenced by favorable environmental conditions, such as the increase of the relative vorticity and the decrease of the vertical wind shear, the high SST and the strengthened vertical velocity (ω). The increase in relative vorticity at the lower layer (850 hPa) can concentrate more convective heating, which is beneficial to the TC development. The vertical wind shear is usually calculated as the difference between wind vectors at 200 hPa and 850 hPa. The decreased vertical wind shear can reduce the advection of heat and moisture from the TC center.

Figure 4 displays a significant enhancement in vertical velocity (ω) in the southeastern part (123° E- 180° , 0° - 13° N) of the WNP between P2 and P3. Increase in relative vorticity can also be found in similar and even larger areas. It can be seen that compared with P2, the SSTs during P3 in the WNP and Indian Ocean increase significantly. The significant statistical results are 95%. Figure 4 also shows that the vertical wind shear in the WNP during P3 period is smaller than that during P2. In summary, according to Fig. 3, the difference of the TC genesis position is associated with the location of atmospheric and SST conditions difference between P3 and P2. Figures 3 and 4 suggest that more TCs could occur during P3 due to the increase in low-level relative vorticity and SST, and also the enhanced vertical convection.

Figures 5–6 display differences in atmospheric and SST conditions between P2 and P3 in La Niña years, El Niño years, respectively. Figure 5 shows that in La Niña years, the vertical velocity, the relative vorticity and the vertical wind shear, which are conducive to the development of TCs, are mainly concentrated between 0° and 18° N, and there is a significant SST increase area. The positions of the positive relative vorticity and negative vertical velocity are very similar to the positions where the number of TCs in Fig. 3 increases. The large-scale climate differences for El Niño years are shown in Fig. 6. The P3 vertical wind shear is smaller than that of P2, which is displayed as a negative value for the WNP basin. Also, there are apparent positive vorticity anomalies between 6° - 18° N, 140° E- 180° . The significant positive SST

differences and negative vertical velocity differences at 2°-12°N and 150°E-180° are beneficial to TC genesis. Figures 5–6 show that the amplitude of SST difference is somewhat dissimilar, which may be one of the reasons why the TC frequency in La Niña years and El Niño years changes differently (Fig. 2).

4.2 Relations to SST variations

According to the above analyses, whatever it is a La Niña year or an El Niño year, the SST plays a role in WNP TCs. As suggested by previous studies (Zhan et al., 2011; Hsu et al., 2014; Yamaguchi et al., 2020), the different SST anomaly distributions can impact atmospheric circulation in the WNP. The SST changes in the WNP region are warm SST differences between P2 and P3 (Figs. 4–6). We calculate the correlation of the WNP TC frequency throughout the year (January-December) with SST over the three ocean basins during 1979–2020 (Fig. 7a). A significant negative correlation appears in the northern Indian Ocean, due to the remote SST warming effect on WNP TCs (Wang et al. 2021). The significant negative correlation in the Atlantic Ocean is related to the AMO (Zhang et al. 2018). The significant positive correlation is seen in the eastern and central Pacific, owing to the ENSO phenomenon. Figure 7b compares the TC frequency throughout the year (January-December) with the Niño 3.4 index. The correlation during 1979–2020 is 0.12, indicating that ENSO is not significantly correlated with the TC number in the whole WNP (e.g., Wang and Chan 2002). The correlations between the Niño 3.4 index and TC frequency during P1, P2 and P3 are – 0.31, 0.22 and 0.38, respectively, all of which are below the 90% significant level.

To emphasize the decadal variations, we perform the 7-year running mean on the data and repeat the correlation calculations (Fig. 8). The patterns of correlation distribution in Fig. 7a and Fig. 8a are similar, indicating that the correlation pattern in Fig. 7a (at both interannual and decadal time scales) is dominated by decadal variability. A significant negative correlation around 36°N can also be seen in Fig. 8a. The correlation patterns in the Pacific are similar to those of the PDO. Therefore, we compare the TC frequency variation at decadal time scales with the PDO index (Fig. 8b). The correlation between the PDO and WNP TC frequency during 1982–2017 is 0.71 with a 99% confidence level. Figure 8b also shows that the decadal relationships of WNP TCs with the PDO are opposite before and after the middle 1990s. The correlations during 1982–1995 and 1996–2017 are – 0.84 and 0.90, respectively. These analyses suggest that in the Pacific, the PDO has a stronger relationship with WNP TCs than ENSO.

4.3 Compared with P1

Based on the above results (Figs. 1 and 8b), P1 and P3 are both in the warm phase of the PDO. The TC frequency during the late season (October-December) or from June to August in P1 has previously been studied (Zhao and Wang, 2016, 2019). In this section, the changes in the factors influencing the TC frequency between P1 and P3 are discussed.

Zhao and Wang (2016, 2019) previously point out that the warm phase (P1) is related to the increase in the TC frequency and the decrease of interannual correlation between ENSO and TCs, while the cold phase (P2) is related to the decrease in the TC frequency and the increase in interannual correlation between ENSO and TCs. The changes of relative vorticity and vertical wind shear in the WNP play a major

role in the change of the TC frequency during P1 compared to P2. The change in SST in tropical Indo-Pacific is closely associated with the correlation between ENSO and TCs. According to the analysis of the P3 period, we find that the WNP TC frequency also increases, which are consistent with the result of P1 (Zhao and Wang, 2016, 2019): the PDO influences the WNP TC frequency. The TC frequency is the highest in neutral years and the smallest in La Niña years (Fig. 2), which is different from P1 described in Zhao and Wang (2016): La Niña years are with the highest TC frequency and El Niño years are with the lowest. The TC frequency in El Niño years is no longer the least during P3. This may be caused by the PDO: the correlation between the TC frequency per year and PDO is different during P1 and P3 (Fig. 8b). In addition, the difference between P1 and P3 may be caused by the warmer SST. The SST gradient between the northern Indian Ocean and WNP influences the South China Sea TC Frequency (Li and Zhou, 2014). The WNP SST during the P3 period is higher than that during P2, which is different from P1. Warm SST anomalies in the WNP are observed during P3 (the warm phase of the PDO), which can induce equatorial wind anomalies and thereby further change atmospheric circulations. Different with P1, during the El Niño years and La Niña years of P3, the WNP TC frequency is mainly affected by vertical wind shear and relative vorticity, as well as by vertical velocity (Figs. 5–6).

Discussion And Conclusions

In this study, the increase in the WNP TC frequency during 2011–2020 is analyzed based on large-scale atmospheric and ocean conditions. During 2011–2020, approximately 26 TCs occurred on average every year in the WNP and caused catastrophic damages to the Philippines and other Asian countries (Fig. 3). In recent years, several studies found a decrease in TC counts during 1979–2010 (Hsu et al., 2014; Zhao and Wang, 2016, 2019). It is associated with ENSO and PDO changes. Previous studies mainly focused on the TC frequency before 2015 and did not investigate the change of the whole year TC frequency after 2015. Such investigations are necessary and useful to improve our understanding of TC activity in the WNP.

Based on the JTWC best-track data, this study examines the variations in the WNP TC frequency between January and December of 1979–2020. The WNP TC count shows a significant decline in 1998 and a rise since 2010, resulting in a low cycle (P2: 1998–2010) and two high cycles (P1: 1979–1997 and P3: 2011–2020). Previous studies have analyzed the decrease between P1 and P2. In this study, the analysis is mainly focused on the increased counts of WNP TCs in P3. A difference in the TC number between P2 and P3 can be found (Figs. 1 and 2). The difference is mainly due to the significant difference in La Niña years and neutral years. During P3, the TC frequency for El Niño years, La Niña years and neutral years are slightly different. Among the three types of years, the TC frequency is the highest in neutral years and the smallest in La Niña years. This is different from P1 described in Zhao and Wang (2016) where La Niña years are the highest and El Niño years are the lowest. There may be two reasons for this: one is the different months used to count TCs, and the other is due to the warm SST during the P3 period compared with P2 period (Fig. 4). Zhao and Wang (2016) used TCs during October to December, whereas the present study analyzed the TC frequency from January to December. Li and Zhou (2014) point out that the zonal SST gradient between the cooling WNP SST and the warming northern Indian Ocean SST is not

favorable for TC genesis. The warming WNP SST during P3 reduces the zonal SST gradient, resulting in a favorable environment for TC genesis (Liu and Chan, 2020).

Our research also suggests that the changes of dynamical factors like low-level vorticity, vertical wind shear and vertical velocity play an essential role in TC genesis during P3. Vertical velocity, relative vorticity and SST play a major role in La Nina years. For El Niño years, relative vorticity, vertical wind shear and SST are dominant. The WNP SST has an important influence on TC activity (Hsu et al. 2014; Song et al. 2020). So we study the correlation between the WNP TC frequency and SST. The result shows that the WNP TC frequency and SST have a significant positive correlation region and a significant negative correlation region. The correlation coefficients distributions in the WNP are related to the PDO pattern at decadal time scales (Fig. 8a). To further confirm the influence of the PDO, we compare the time series of the PDO and TC frequency (Fig. 8b). The calculation indicates that the PDO is positively correlated to the frequency of TC. The correlation coefficient is 0.71, which is significant at 99% confidence level.

P1 and P3 are both in the warm phase of the PDO. Compared with P2, the tropical Pacific SST of P3 is warmer, and P1 is colder (Zhao and Wang, 2016). This may be one of the reasons why the average TC frequency is different during P3 and P1. The warmer phase of the PDO with warmer WNP SST anomalies is a favorable environmental factor for TC genesis. To sum up, warmer SST during the warm phase of the PDO may cause atmospheric circulation anomalies in the WNP which in turn affect TC activity.

In summary, more TCs are detected during P3 compared with P2. During the period 2011–2020, the warm phase of the PDO and the warm tropical Pacific SST are favorable for increasing the TC frequency in the WNP. SST anomalies could change atmospheric circulations. The large-scale atmospheric environmental conditions like relative vorticity, vertical wind shear and vertical velocity play a significant role in TC genesis during P3. The PDO plays an important role on the whole year TC activity in the WNP. Under global warming environmental conditions, this article provides a better outlook of TC activity in the WNP.

Declarations

Acknowledgments

This study is supported by the National Natural Science Foundation of China (41731173), the National Key R&D Program of China (2019YFA0606701), the Strategic Priority Research Program of the Chinese Academy of Sciences (XDB42000000 and XDA20060502), the Key Special Project for Introduced Talents Team of Southern Marine Science and Engineering Guangdong Laboratory (Guangzhou) (GML2019ZD0306), the Innovation Academy of South China Sea Ecology and Environmental Engineering, the Chinese Academy of Sciences (ISEE2021ZD01), and the Leading Talents of Guangdong Province Program. The numerical simulation is supported by the High Performance Computing Division in the South China Sea Institute of Oceanology.

References

1. Bister M, Emanuel KA (1997) The genesis of Hurricane Guillermo: TEXMEX analyses and a modeling study. *Mon Weather Rev* 125:2662–2682. [https://doi.org/10.1175/1520-0493\(1997\)125<2662:TGOHGT>2.0.CO;2](https://doi.org/10.1175/1520-0493(1997)125<2662:TGOHGT>2.0.CO;2)
2. Choi JW, Kim HD (2019) Negative relationship between Korea landfalling tropical cyclone activity and Pacific Decadal Oscillation. *Dyn Atmos Ocean* 87:101100. <https://doi.org/10.1016/j.dynatmoce.2019.101100>
3. Choi Y, Ha KJ, Ho CH, Chung CE (2015) Interdecadal change in typhoon genesis condition over the western North Pacific. *Clim Dyn* 45:3243–3255. <https://doi.org/10.1007/s00382-015-2536-y>
4. He H, Yang J, Gong D et al (2015) Decadal changes in tropical cyclone activity over the western North Pacific in the late 1990s. *Clim Dyn* 45:3317–3329. <https://doi.org/10.1007/s00382-015-2541-1>
5. Hsu PC, Chu PS, Murakami H, Zhao X (2014) An abrupt decrease in the late-season typhoon activity over the Western North Pacific. *J Clim* 27:4296–4312. <https://doi.org/10.1175/JCLI-D-13-00417.1>
6. Huang B, Thorne PW, Banzon VF et al (2017) Extended reconstructed Sea surface temperature, Version 5 (ERSSTv5): Upgrades, validations, and intercomparisons. *J Clim* 30:8179–8205. <https://doi.org/10.1175/JCLI-D-16-0836.1>
7. Kalnay E, Kanamitsu M, Kistler R, et al (1996) The NCEP/NCAR 40-Year Reanalysis Project. *Bull Am Meteorol Soc* 77:437–471. [https://doi.org/10.1175/1520-0477\(1996\)077<0437:TNYRP>2.0.CO;2](https://doi.org/10.1175/1520-0477(1996)077<0437:TNYRP>2.0.CO;2)
8. Kim HM, Webster PJ, Curry JA (2011) Modulation of North Pacific tropical cyclone activity by three phases of ENSO. *J Clim* 24:1839–1849. <https://doi.org/10.1175/2010JCLI3939.1>
9. Kim JH, Ho CH, Kim HS et al (2008) Systematic variation of summertime tropical cyclone activity in the western North Pacific in relation to the Madden-Julian oscillation. *J Clim* 21:1171–1191. <https://doi.org/10.1175/2007JCLI1493.1>
10. Knutson TR, McBride JL, Chan J et al (2010) Tropical cyclones and climate change. *Nat Geosci* 3:157–163. <https://doi.org/10.1038/ngeo779>
11. Li RCY, Zhou W (2013) Modulation of western north pacific tropical cyclone activity by the ISO. Part I: Genesis and intensity. *J Clim* 26:2904–2918. <https://doi.org/10.1175/JCLI-D-12-00210.1>
12. Li RCY, Zhou W (2014) Interdecadal change in South China Sea tropical cyclone frequency in association with zonal sea surface temperature gradient. *J Clim* 27:5468–5480. <https://doi.org/10.1175/JCLI-D-13-00744.1>
13. Lin II, Chan JCL (2015) Recent decrease in typhoon destructive potential and global warming implications. *Nat Commun* 6:. <https://doi.org/10.1038/ncomms8182>
14. Liu C, Zhang W, Geng X et al (2019) Modulation of tropical cyclones in the southeastern part of western North Pacific by tropical Pacific decadal variability. *Clim Dyn* 53:4475–4488. <https://doi.org/10.1007/s00382-019-04799-w>
15. Liu KS, Chan JCL (2020) Recent increase in extreme intensity of tropical cyclones making landfall in South China. *Clim Dyn* 55:1059–1074. <https://doi.org/10.1007/s00382-020-05311-5>

16. Liu KS, Chan JCL, Kubota H (2021) Meridional oscillation of tropical cyclone activity in the western North Pacific during the past 110 years. *Clim Change* 164:. <https://doi.org/10.1007/s10584-021-02983-8>
17. Mei W, Xie SP (2016) Intensification of landfalling typhoons over the northwest Pacific since the late 1970s. *Nat Geosci* 9:753–757. <https://doi.org/10.1038/ngeo2792>
18. Mendelsohn R, Emanuel K, Chonabayashi S, Bakkensen L (2012) The impact of climate change on global tropical cyclone damage. *Nat Clim Chang* 2:205–209. <https://doi.org/10.1038/nclimate1357>
19. Molinari J, Vollaro D, Skubis S, Dickinson M (2000) Origins and mechanisms of eastern Pacific tropical cyclogenesis: A case study. *Mon Weather Rev* 128:125–139. [https://doi.org/10.1175/1520-0493\(2000\)128<0125:OAMOEP>2.0.CO;2](https://doi.org/10.1175/1520-0493(2000)128<0125:OAMOEP>2.0.CO;2)
20. Nolan DS, Rappin ED, Emanuel KA (2007) Tropical cyclogenesis sensitivity to environmental parameters in radiative-convective equilibrium. *Q J R Meteorol Soc* 133:2085–2107. <https://doi.org/10.1002/qj.170>
21. Peduzzi P, Chatenoux B, Dao H et al (2012) Global trends in tropical cyclone risk. *Nat Clim Chang* 2:289–294. <https://doi.org/10.1038/nclimate1410>
22. Rayner NA, Parker DE, Horton EB et al (2003) Global analyses of sea surface temperature, sea ice, and night marine air temperature since the late nineteenth century. *J Geophys Res Atmos* 108:. <https://doi.org/10.1029/2002jd002670>
23. Ritchie EA, Holland GJ (1997) Scale interactions during the formation of typhoon irving. *Mon Weather Rev* 125:1377–1396. [https://doi.org/10.1175/1520-0493\(1997\)125<1377:SIDTFO>2.0.CO;2](https://doi.org/10.1175/1520-0493(1997)125<1377:SIDTFO>2.0.CO;2)
24. Song J, Duan Y, Klotzbach PJ (2020) Increasing trend in rapid intensification magnitude of tropical cyclones over the western North Pacific. *Environ Res Lett* 15:. <https://doi.org/10.1088/1748-9326/ab9140>
25. Timmermann A, An S, Il, Kug JS et al (2018) El Niño–Southern Oscillation complexity. *Nature* 559:535–545. <https://doi.org/10.1038/s41586-018-0252-6>
26. Trenberth KE, Caron JM (2000) The southern oscillation revisited: Sea level pressures, surface temperatures, and precipitation. *J Clim* 13:4358–4365. [https://doi.org/10.1175/1520-0442\(2000\)013<4358:TSORSL>2.0.CO;2](https://doi.org/10.1175/1520-0442(2000)013<4358:TSORSL>2.0.CO;2)
27. Tu JY, Chou C, Chu PS (2009) The abrupt shift of typhoon activity in the vicinity of Taiwan and its association with western North Pacific-East Asian climate change. *J Clim* 22:3617–3628. <https://doi.org/10.1175/2009JCLI2411.1>
28. Vecchi GA, Soden BJ (2007) Effect of remote sea surface temperature change on tropical cyclone potential intensity. *Nature* 450:1066–1070. <https://doi.org/10.1038/nature06423>
29. Vu T, Kieu C, Chavas D, Wang Q (2020) A Numerical Study of the Global Formation of Tropical Cyclones. *J Adv Model Earth Syst* 1–33. <https://doi.org/10.1029/2020ms002207>
30. Walsh KJE, Sharmila S, Thatcher M et al (2020) Real world and tropical cyclone world. Part II: Sensitivity of tropical cyclone formation to uniform and meridionally varying sea surface

- temperatures under aquaplanet conditions. *J Clim* 33:1473–1486. <https://doi.org/10.1175/JCLI-D-19-0079.1>
31. Wang B, Chan JCL (2002) How strong ENSO events affect tropical storm activity over the western North Pacific. *J Clim* 15:1643–1658. [https://doi.org/10.1175/1520-0442\(2002\)015<1643:HSEEAT>2.0.CO;2](https://doi.org/10.1175/1520-0442(2002)015<1643:HSEEAT>2.0.CO;2)
 32. Wang C, Wu K, Wu L et al (2021) What Caused the Unprecedented Absence of Western North Pacific Tropical Cyclones in July 2020? *Geophys Res Lett* 48:1–9. <https://doi.org/10.1029/2020GL092282>
 33. Wang Q, Li J, Li Y et al (2018) Modulation of tropical cyclogenesis location and frequency over the Indo-western North Pacific by the intraseasonal Indo-western Pacific convection oscillation during the boreal extended summer. *J Clim* 31:1435–1450. <https://doi.org/10.1175/JCLI-D-17-0085.1>
 34. Wang X, Wang C, Zhang L, Wang X (2015) Multidecadal variability of tropical cyclone rapid intensification in the Western North Pacific. *J Clim* 28:3806–3820. <https://doi.org/10.1175/JCLI-D-14-00400.1>
 35. Yamaguchi M, Chan JCL, Moon IJ et al (2020) Global warming changes tropical cyclone translation speed. *Nat Commun* 11:1–7. <https://doi.org/10.1038/s41467-019-13902-y>
 36. Yokoi S, Takayabu YN (2013) Attribution of decadal variability in tropical cyclone passage frequency over the western north pacific: A new approach emphasizing the genesis location of cyclones. *J Clim* 26:973–987. <https://doi.org/10.1175/JCLI-D-12-00060.1>
 37. Zhan R, Wang Y, Wu CC (2011) Impact of SSTA in the East Indian Ocean on the frequency of Northwest Pacific tropical cyclones: A regional atmospheric model study. *J Clim* 24:6227–6242. <https://doi.org/10.1175/JCLI-D-10-05014.1>
 38. Zhan R, Wang Y, Ying M (2012) Seasonal Forecasts of Tropical Cyclone Activity Over the Western North Pacific: A Review. *Trop Cyclone Res Rev* 1:307–324. <https://doi.org/10.6057/2012TCRR03.07>
 39. Zhang G, Zeng G, Li C, Yang X (2020) Impact of PDO and AMO on interdecadal variability in extreme high temperatures in North China over the most recent 40-year period. *Clim Dyn* 54:3003–3020. <https://doi.org/10.1007/s00382-020-05155-z>
 40. Zhang Q, Wu L, Liu Q (2009) Tropical cyclone damages in China 1983–2006. *Bull Am Meteorol Soc* 90:489–495. <https://doi.org/10.1175/2008BAMS2631.1>
 41. Zhang W, Vecchi GA, Murakami H et al (2018) Dominant Role of Atlantic Multidecadal Oscillation in the Recent Decadal Changes in Western North Pacific Tropical Cyclone Activity. *Geophys Res Lett* 45:354–362. <https://doi.org/10.1002/2017GL076397>
 42. Zhang W, Vecchi GA, Villarini G et al (2017) Modulation of western North Pacific tropical cyclone activity by the Atlantic Meridional Mode. *Clim Dyn* 48:631–647. <https://doi.org/10.1007/s00382-016-3099-2>
 43. Zhao H, Wang C (2019) On the relationship between ENSO and tropical cyclones in the western North Pacific during the boreal summer. *Clim Dyn* 52:275–288. <https://doi.org/10.1007/s00382-018-4136-0>

44. Zhao H, Wang C (2016) Interdecadal modulation on the relationship between ENSO and typhoon activity during the late season in the western North Pacific. *Clim Dyn* 47:315–328. <https://doi.org/10.1007/s00382-015-2837-1>
45. Zhao J, Zhan R, Wang Y, Xu H (2018) Contribution of the interdecadal pacific oscillation to the recent abrupt decrease in tropical cyclone genesis frequency over the Western North Pacific since 1998. *J Clim* 31:8211–8224. <https://doi.org/10.1175/JCLI-D-18-0202.1>
46. Zhao K, Zhao H, Raga GB et al (2021) Changes in extended boreal summer tropical cyclogenesis associated with large-scale flow patterns over the western North Pacific in response to the global warming hiatus. *Clim Dyn* 56:515–535. <https://doi.org/10.1007/s00382-020-05486-x>

Figures

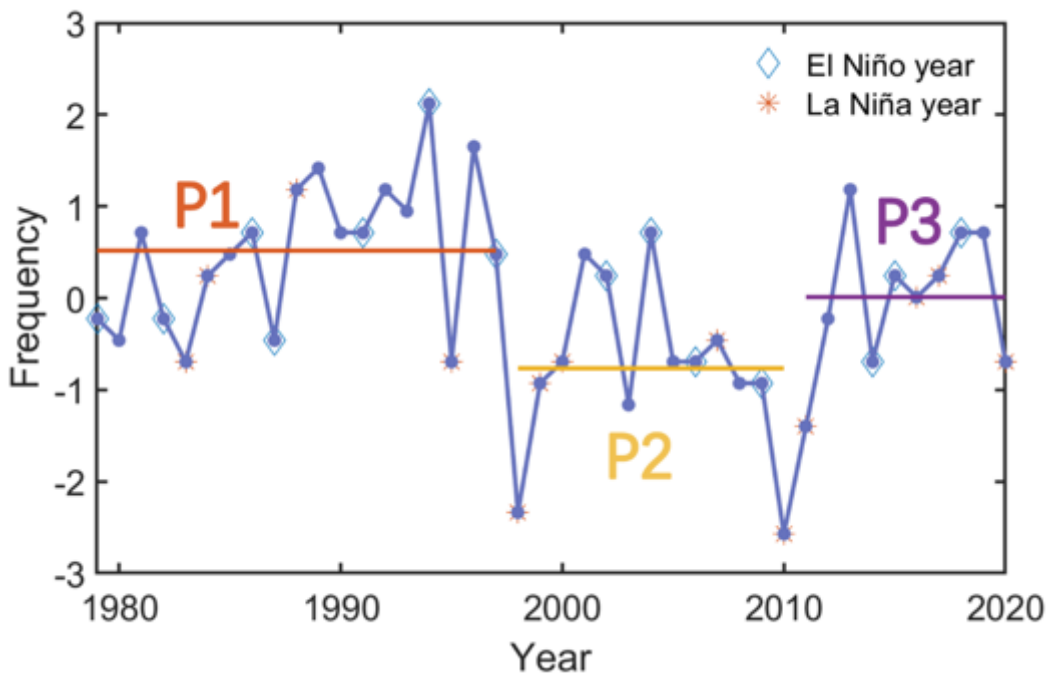


Figure 1

Time series of standardized TC frequency in the WNP. El Niño years and La Niña years are represented with the blue diamond box and orange asterisk, respectively. The orange, yellow and amethyst lines represent the average standardized frequency of TCs in P1 (1979-1997), P2 (1998-2010) and P3 (2011-2020), respectively.

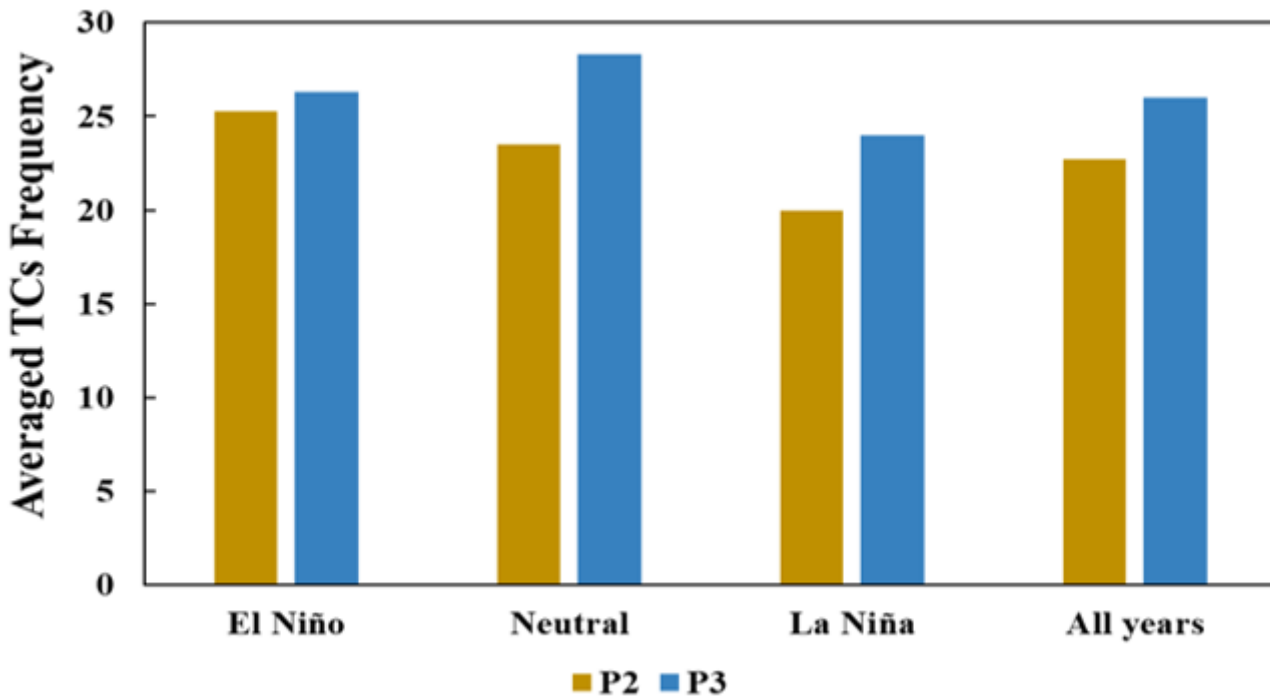


Figure 2

Mean TC number during El Niño years, neutral years, La Niña years and total years for P2 (1998-2010) and P3 (2011–2020).

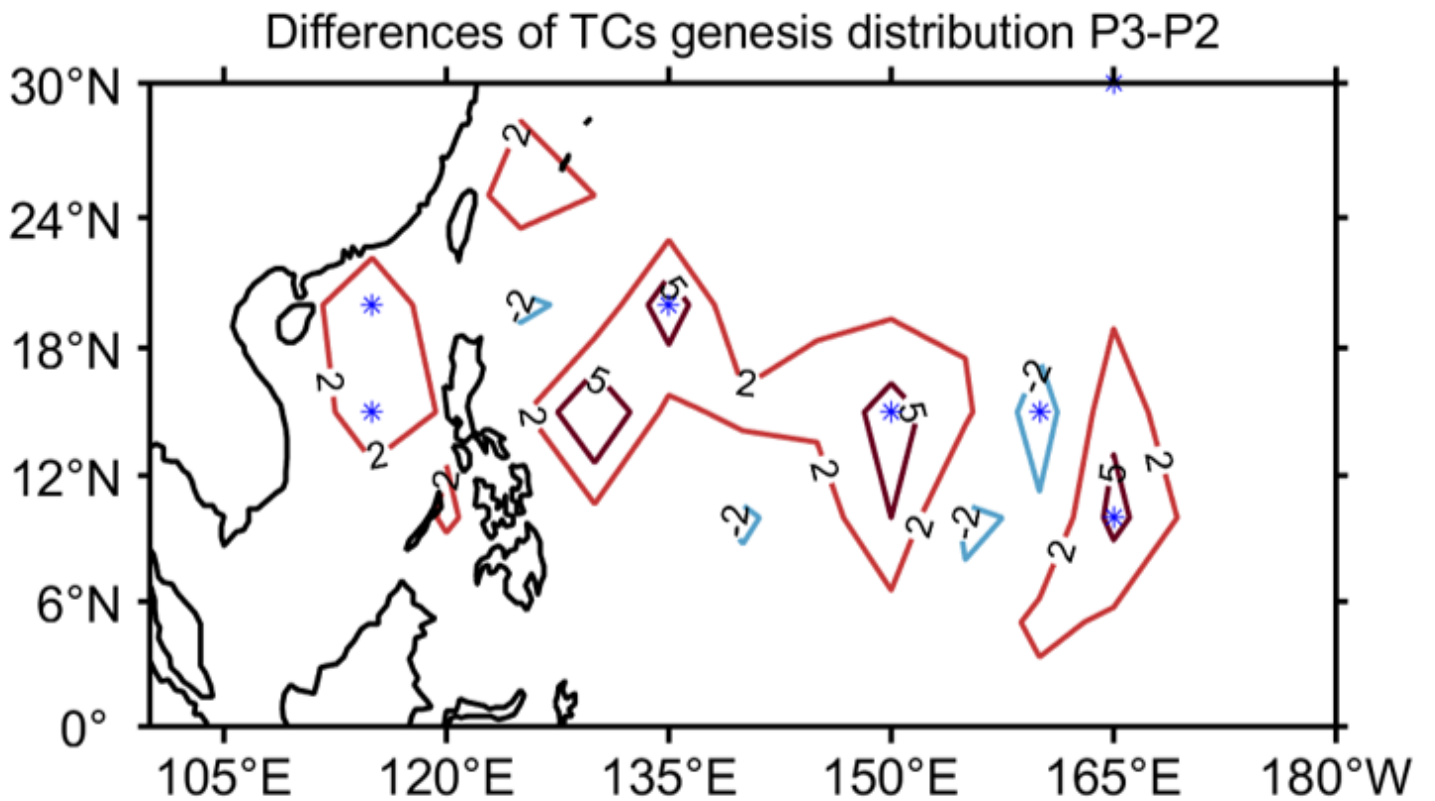


Figure 3

Differences in WNP TC genesis distribution ($\times 10$) between P2 and P3 (P3 minus P2). The asterisk indicates that the statistical difference in this region is significant at 90% confidence level.

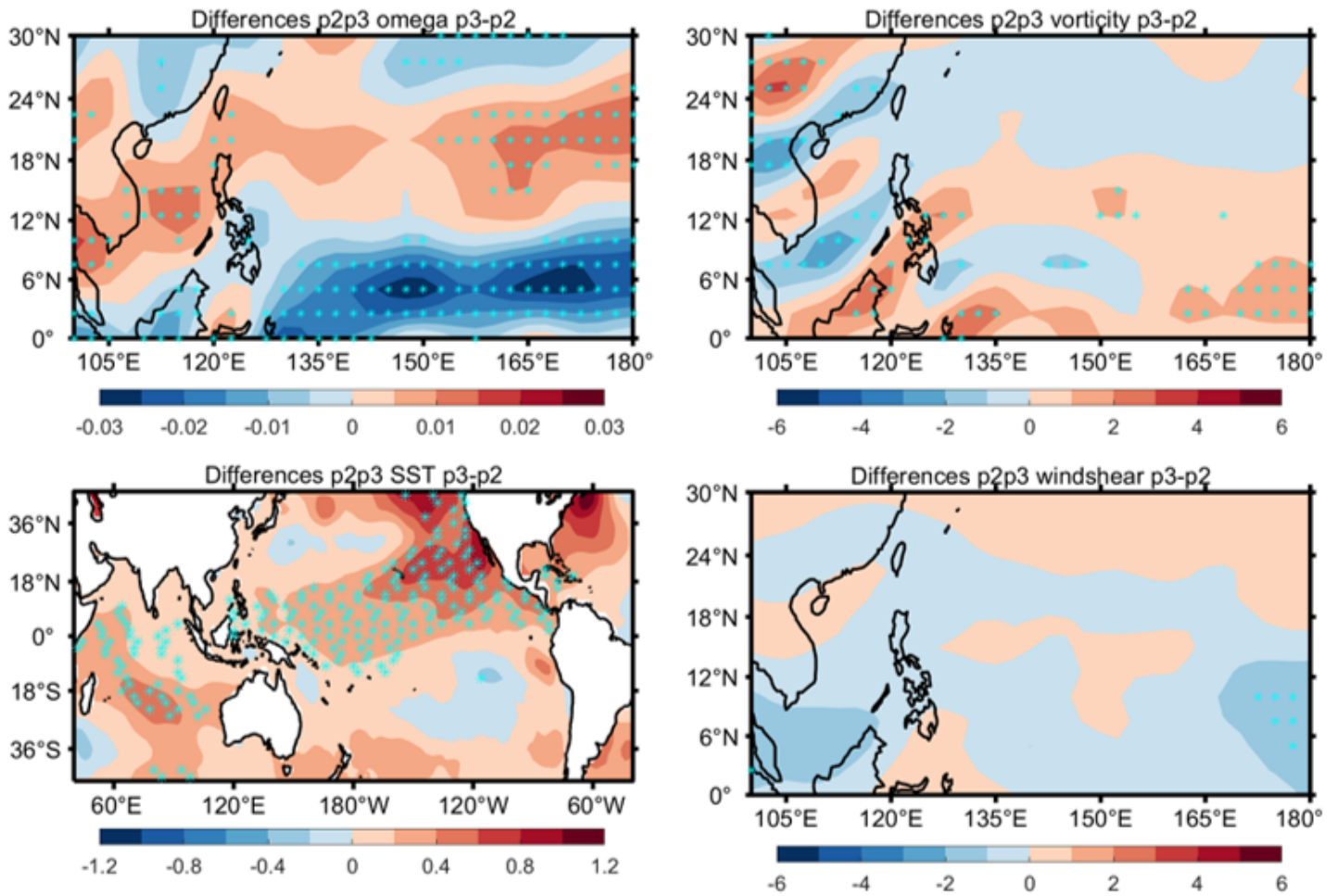


Figure 4

(From left to right and top to bottom) 500 hPa omega difference, 850 hPa relative vorticity difference ($\times 106$), sea surface temperature difference and vertical wind shear difference between P2 and P3 (P3 minus P2). The asterisk indicates that the statistical difference in this region is significant at 95% confidence level.

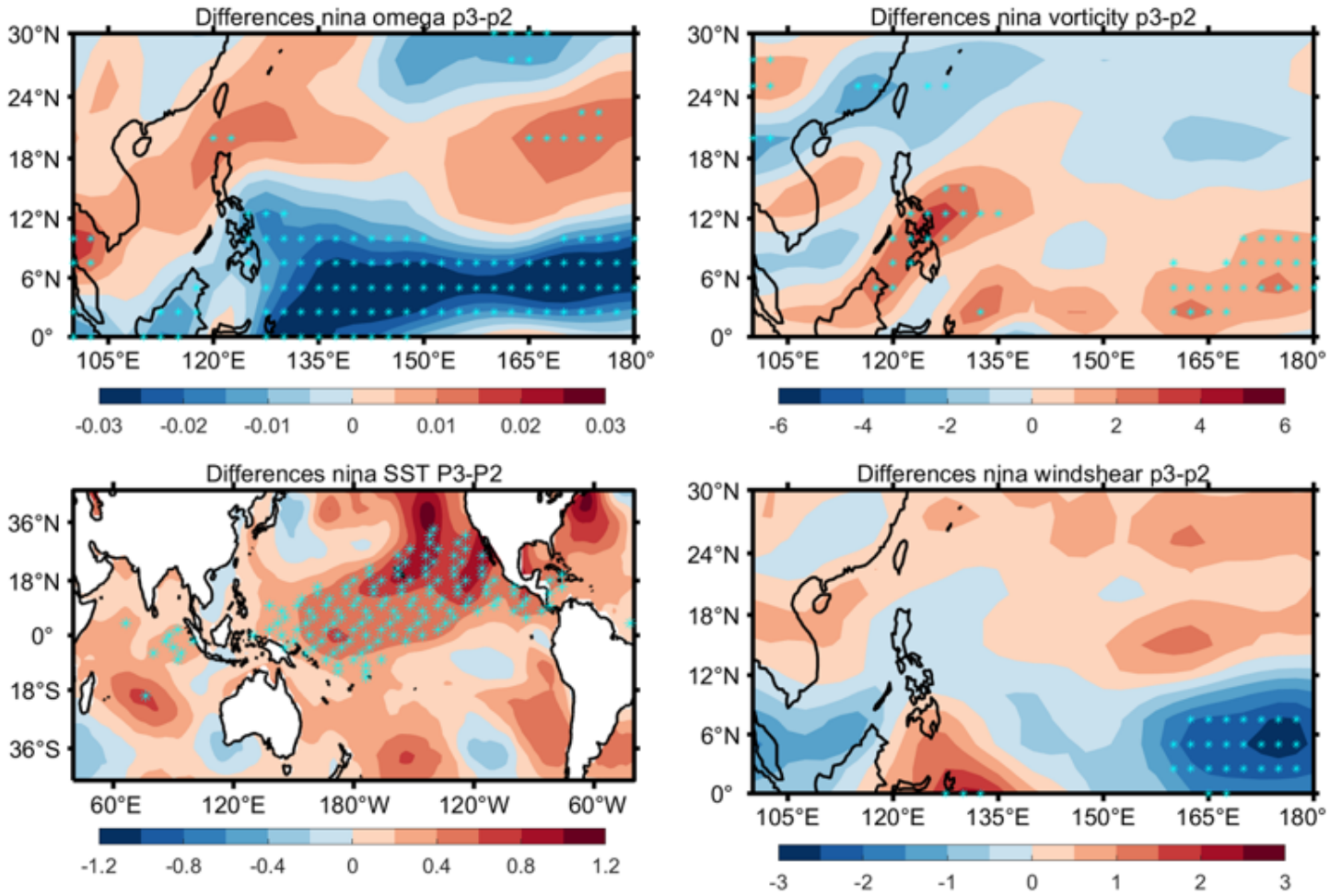


Figure 5

Same as Figure 4, but the differences are for La Niña years.

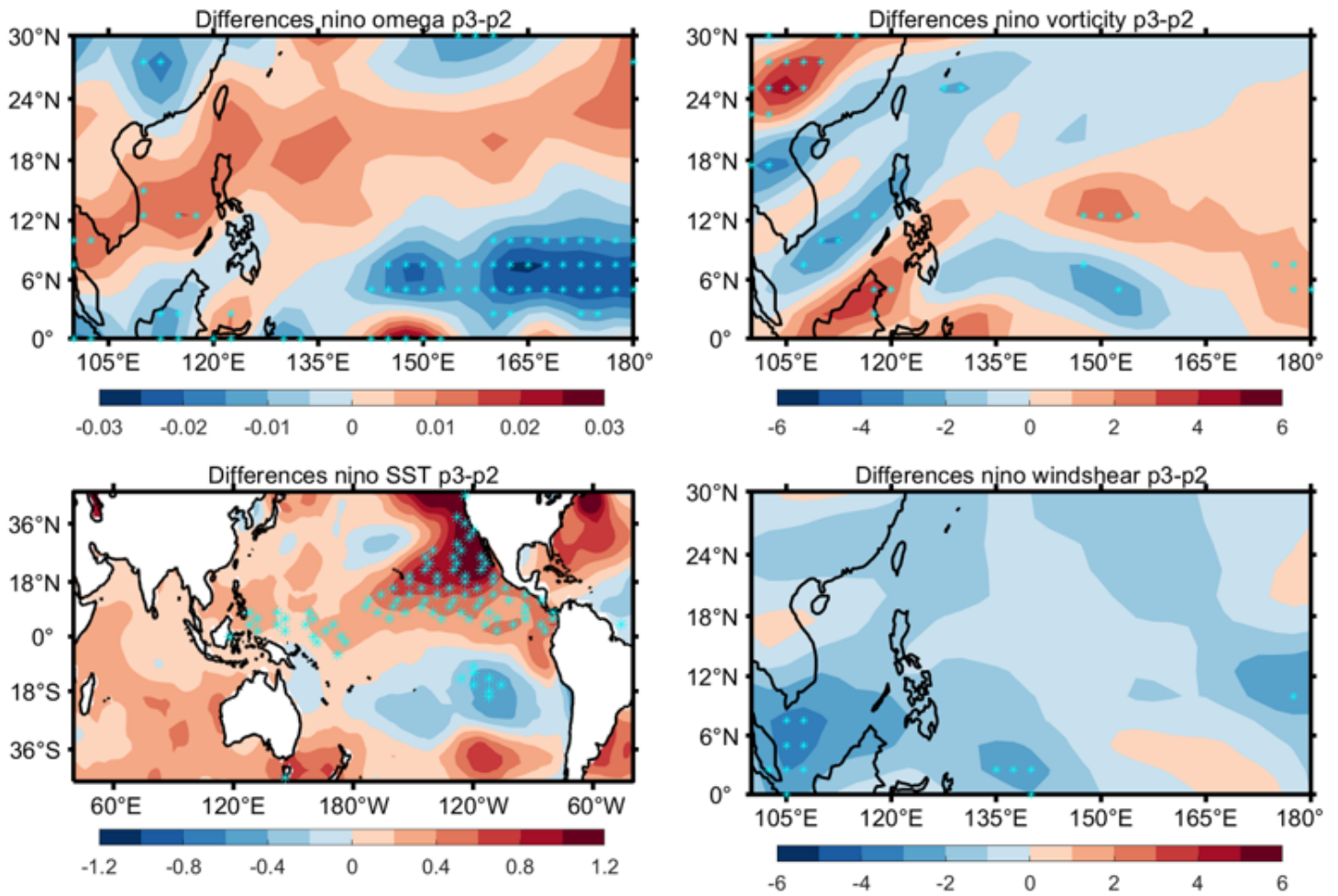


Figure 6

Same as Figure 4, but the differences are for El Niño years.

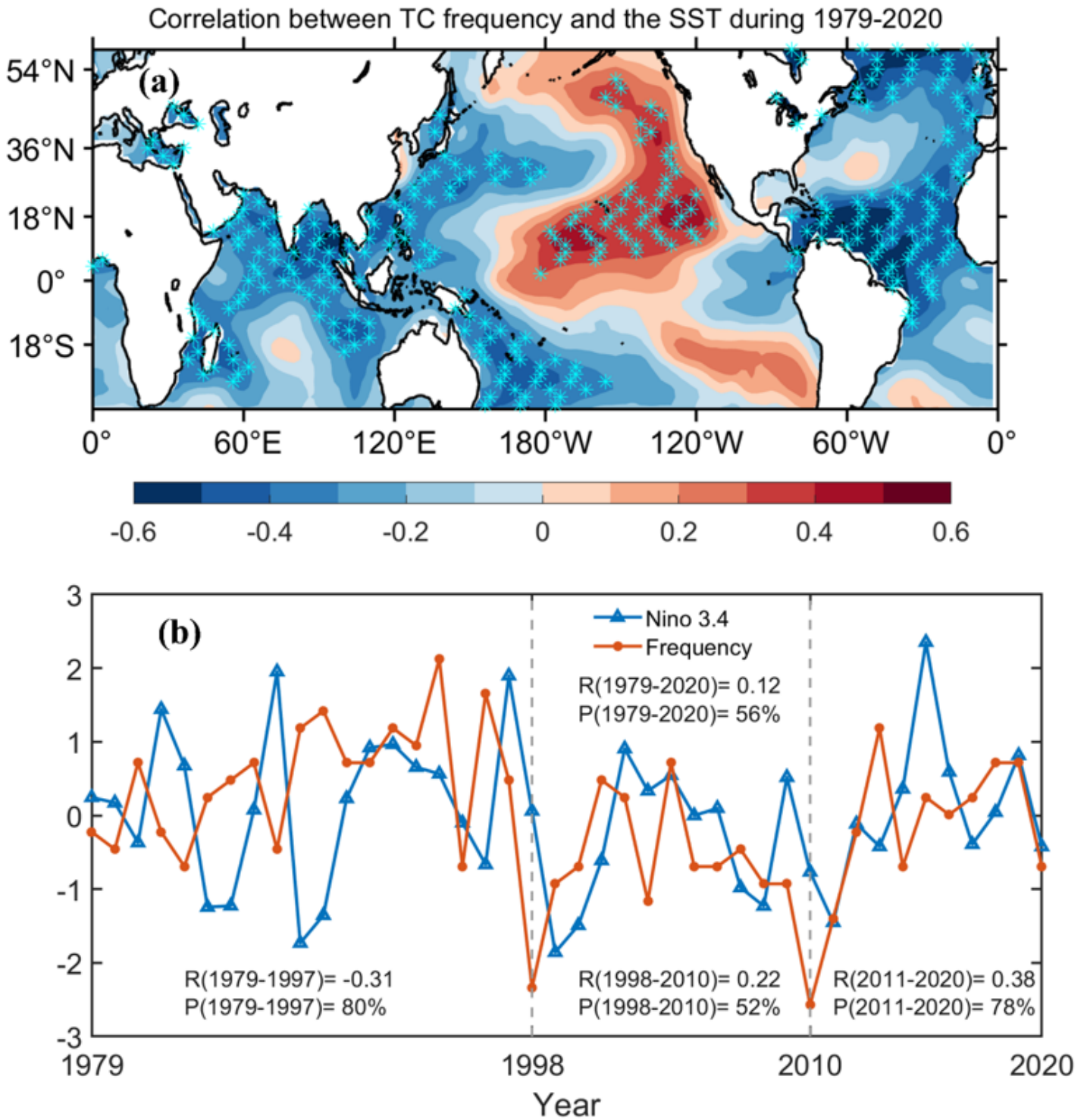


Figure 7

(a) Correlation between the TC frequency and SST during 1979-2020. The asterisk indicates statistical significance at 95% confidence level. (b) Time series of the Niño 3.4 index (blue line) and the TC frequency (orange line), both of which are standardized. During 1979-2020, the correlation is 0.12. During P1, P2 and P3, the correlations between the Niño 3.4 and the TC frequency are -0.31, 0.22 and 0.38, respectively.

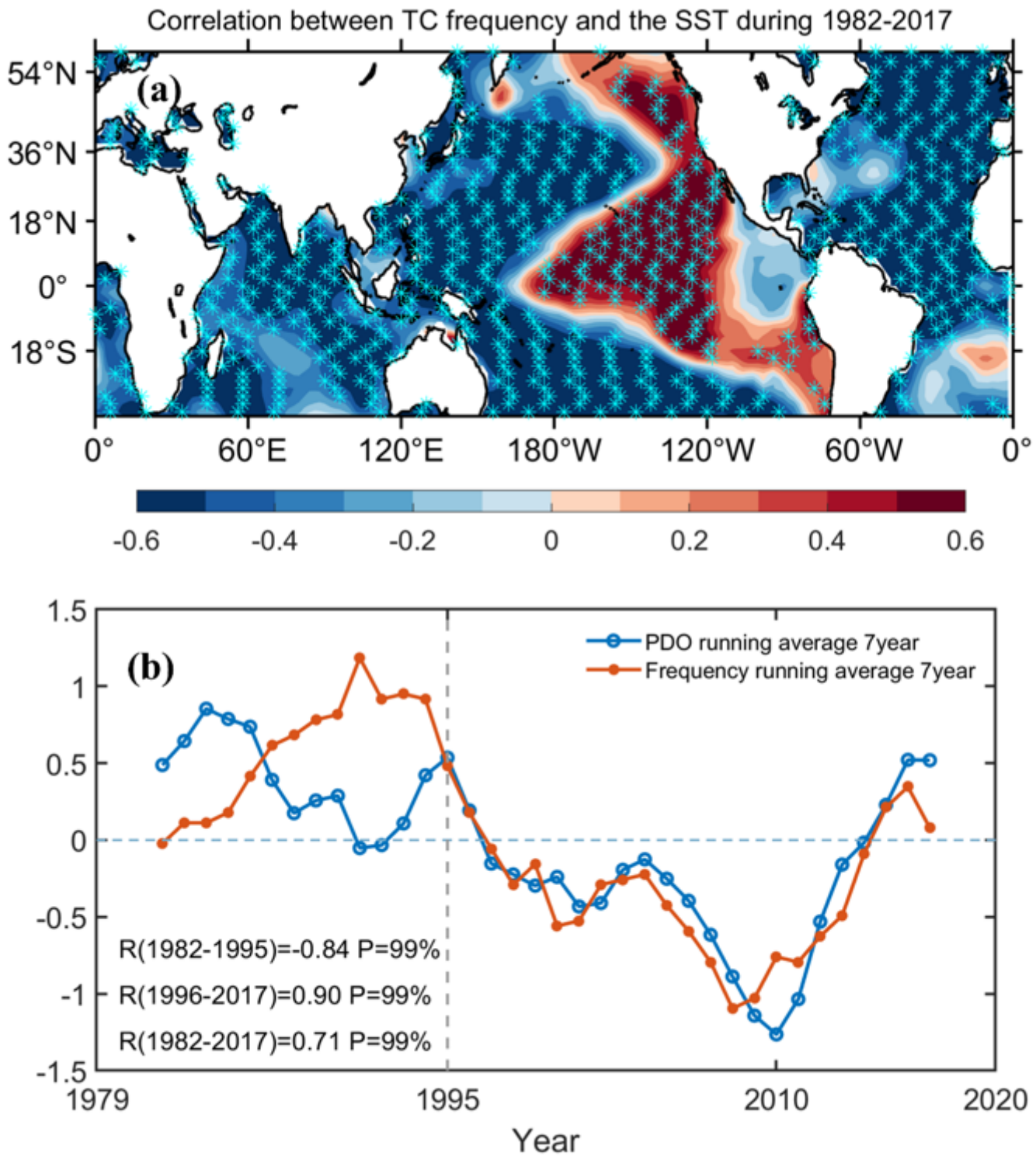


Figure 8

(a) Correlations between the TC frequency and SST during 1982-2017 at decadal time scales. The asterisk indicates statistical significance at 95% confidence level. (b) Time series of the PDO index (blue line) and the TC frequency (orange line). The TC frequency and the PDO index are standardized. During 1982-1995 and 1996-2017, the correlation between the PDO and the TC frequency is -0.84 and 0.9,

respectively. The correlation of the whole interval from 1982 to 2017 is 0.71. A 7-year running mean is performed on all data to obtain decadal variability.